Supporting Information for the manuscript:

Multi-Stimuli Chromic Responses (Light/Electro/Amino-) in Zn/Cd-Extended Viologen Materials toward Information Encryption

Chen-Ran Zhang,[1] Ming Xiao,[1] Qun-Shan Ding,[1,2] Lin-Ke Li[*,1], Xue-Li Zhao,[1] Shuang-Quan Zang[1]

1. *Henan Key Laboratory of Crystalline Molecular Functional Materials, College of Chemistry and Pingyuan Laboratory, Zhengzhou University, Zhengzhou 450001, P. R. China*
2. *Zhengzhou Zhengshi Chemical Co., Ltd, Zhengzhou 450002, P. R. China*

This file includes Tables S1-S6 and Figs. S1−S20

Experimental Section

Measurements

All reagents were purchased from commercial sources and used without further purification. Powder X-ray diffraction (PXRD) data were collected at 293 K using a Rigaku D/max-3B diffractometer with Cu Kα radiation (λ = 1.5418 Å). The single-crystal sample was ground and scanned from 5-50° with a step size of 0.1°. Infrared (IR) spectra were recorded on a Burker VECTOR 22 spectrometer in the range of 4000-400 cm^{-1} using the KBr pellet method. Thermogravimetric analysis (TGA) was carried out on a TA Q50 thermal analyzer under a nitrogen atmosphere with a heating rate of 10 °C/min from room temperature to 800

°C. Electron paramagnetic resonance (EPR) signals were measured at room temperature using a Bruker A300 spectrometer. Solid-state ultraviolet-visible diffuse reflectance spectroscopy (UV-Vis DRS) data were collected in the 200-800 nm wavelength range using a JASCO UVDEC-660 spectrophotometer.

Crystal structure determination

Single crystal X-ray analyses were conducted on a Bruker SMART APEX CCD diffractmeter using graphite-monochromatized Cu-Kα radiation (λ = 1.54178 Å) at 200K using the ω-scan technique. Lorentz polarization and absorption corrections were applied. The structures were solved by direct methods with SHELXS-97[S1] and refined by full-matrix least-squares using the SHELXL-97 program[S2]. All non-hydrogen atoms were refined anisotropically. The hydrogen atoms of ligands were included in the structure factor calculations in a riding model at idealized positions and refined isotropically. Hydrogen atoms of solvent molecules were located from difference Fourier maps, then their positions were fixed and refined isotropically. For compounds **1** and **2**, the guest water molecules exhibit a high degree of disorder and cannot be reasonably modeled. Therefore, the SQUEEZE routine of the PLATON program was employed to remove the diffuse electron densities arising from these solvent molecules, thereby yielding solvent-free diffraction intensity data[S3]. The content of the guest molecules was quantified through elemental analysis and thermogravimetric analysis, which ultimately enabled the determination of the molecular formulae for **1** and **2**.

Crystallographic data and selected bond lengths and angles for the two compounds are listed in Tables S1-S6.

Computational Details

The calculations were carried out using density functional theory with the PBE form of generalized gradient approximation functional (GGA)[S4]. The Vienna ab-initio simulation package (VASP)[S5-S8] was employed. The plane wave energy cutoff was set as 400 eV. The Fermi scheme was employed for electron occupancy with an energy smearing of 0.1 eV. The first Brillouin zone was sampled in the Monkhorst−Pack grid[S9]. The 4×4×3 k-point mesh for the bulk calculation. The energy (converged to 1.0 ×10-6 eV/atom) and force (converged to 0.01eV/Å) were set as the convergence criterion for geometry optimization. The van der Waals (vdW) interaction was described by a semiempirical DFT-D3 force-field approach[S10,

[S11]. The spin polarization was considered in all calculation.

Synthesis of 4,4'-(sulfonylbis(4,1-phenylene))bis(1-(4-carboxybenzyl)pyridin-1-ium) chloride [(H_2L)·2Cl]

The core of ligand (H_2L)·Cl_2 was prepared by Suzuki-Miyaura Cross Coupling reaction. In a three-necked flask, Bis(4-chlorophenyl) sulphone (0.862 g, 3 mmol), K_2CO_3 (0.995 g, 7.2 mmol), 4-Pyridylboronic acid (0.885 g, 7.2 mmol), Tetrakis(triphenylphosphine)palladium (0.289 g, 0.25 mmol) and H_2O/EtOH/1,4-Dioxane (1:1:3) were added and stirred at 100 ℃ in N_2 atmosphere for 24 h. After cooled to room temperature, the reaction mixture was filtered and extracted with CH_2Cl_2. And then, the CH_2Cl_2 layer was concentrated under reduced pressure to afford a yellow solid, which was then purified by column chromatography using a mixture of dichloromethane and methanol (90:10) as the eluent to yield a yellow solid (0.930 g, 83.23 %). Subsequently, the light yellow solid (2.5 mmol), 4-(Chloromethyl)benzoic acid (0.887 g, 5.2 mmol) and DMF (60 mL) was added in a 100 mL flask and stirred in 110 ℃. After 12h, a white powder is generated. Filter the reaction mixture under vacuum to obtain the final product (H_2L)·Cl_2 .Yield 37.4 %. 1H NMR (600MHz CD_3OD): δ 5.97 (s 4H), δ 7.63 (d 4H), δ 8.12(d 4H), δ 8.21 (d 4H), δ 8.28 (d 4H), δ 8.49 (d 4H), δ 9.16 (d 4H).

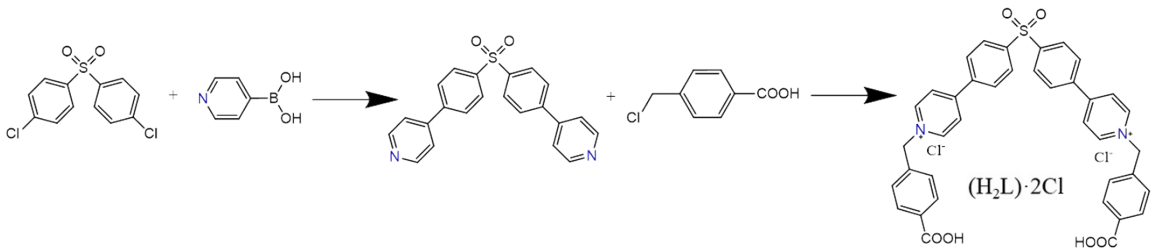

Cyclic voltammetry

In a 1.5 mL centrifuge tube, 15 mg of the ground sample powder and 1.5 mg of PVDF binder were added, followed by the addition of 100 μL of *N*-methyl-2-pyrrolidone (NMP) solvent. The mixture was then ultrasonic for 30 minutes to form a smooth suspension. Subsequently, use a pipette to evenly coat the well-dispersed mixture onto the conductive side of the ITO glass and control the coating thickness carefully to ensure the uniformity of the film. Finally, place the coated ITO glass on a 60°C hot plate to remove residual solvent. Cyclic voltammetry (CV) measurements were carried out on a CHI760 electrochemical workstation using a standard three-electrode system. The modified ITO glass, platinum mesh,

and saturated Ag/AgCl electrode were used as the working electrode, counter electrode, and reference electrode, respectively. A 0.15 M Na_2SO_4 solution was employed as the electrolyte, with a scan rate of 50 mV/s.

Table S1 Crystallographic Data for Compound **1**

Compound	**1**
Empirical formula	$C_{46}H_{42}ZnN_2O_{14.5}S$
Formula weight	951.24
Temperature / K	200.00(10)
Crystal system	triclinic
Space group	P-1
a / Å	9.52710(10)
b / Å	13.7081(2)
c / Å	16.4123(3)
α / °	91.3780(10)
β / °	99.7860(10)
γ / °	101.9110(10)
Volume / Å^3	2062.87(5)
Z	2
ρ_{calc} g / cm^3	1.531
μ / mm^{-1}	1.956
F (000)	986.0
Radiation	Cu Kα (λ = 1.54184)
θ range for data collection / °	5.474 to 147.626
Index ranges	$-10 \le h \le 11$, $-16 \le k \le 16$, $-19 \le l \le 20$
Reflections collected	20289
Independent reflections	8062 [R_{int} = 0.0344, R_{sigma} = 0.0404]
Data / restraints / parameters	8062 / 0 / 579
Goodness-of-fit on F^2	1.048
Final R indexes [$I >= 2\sigma(I)$]	R_1=0.0518, $_wR_2$=0.1350
Final R indexes [all data]	R_1=0.0604, $_wR_2$=0.1402
Largest diff. peak / hole / e Å^{-3}	1.09 / -0.84

$R_1 = \sum||F_o|-|F_c||/\sum|F_o|$. $wR_2 = [\sum w(F_o^2 - F_c^2)^2/\sum w(F_o^2)^2]^{1/2}$

Table S2 Selected Bond Distances for **1**

Bond	**Length/Å**	**Bond**	**Length/Å**
Zn1-O2[1]	1.9961(19)	Zn1-O6	1.9935(19)
Zn1-O7	2.265(2)	Zn1-O8	2.014(2)
Zn1-O11[2]	2.076(2)		

Table S3 Selected Bond Angles for **1**

Bonds	**Angle /°**	**Bonds**	**Angle /°**
O6-Zn1-O2[1]	109.86(9)	O7-Zn1-O2[1]	89.02(9)
O7-Zn1-O6	93.00(9)	O8-Zn1-O2[1]	107.14(11)
O8-Zn1-O6	142.95(10)	O8-Zn1-O7	85.65(9)
O11[2]-Zn1-O2[1]	87.49(8)	O11[2]-Zn1-O6	95.06(8)
O11[2]-Zn1-O7	171.90(9)	O11[2]-Zn1-O8	88.40(9)

Table S4 Crystallographic Data for Compound **2**

Compound	**2**
Empirical formula	$C_{43}H_{42}CdN_2O_{16}S$
Formula weight	987.24
Temperature / K	200.00(10)
Crystal system	triclinic
Space group	P-1
a / Å	9.22150(10)
b / Å	13.5848(2)
c / Å	17.1714(3)
α / °	93.4060(10)
β / °	95.0740(10)
γ / °	105.8870(10)
Volume / Å^3	2052.96(5)
Z	2
ρ_{calc} g / cm^3	1.597
μ / mm^{-1}	5.414
F (000)	1012.0
Radiation	Cu Kα (λ = 1.54184)
2θ range for data collection / °	5.186 to 156.292
Index ranges	-11 ≤ h ≤ 9, -17 ≤ k ≤ 16, -21 ≤ l ≤ 21
Reflections collected	25235
Independent reflections	8226 [R_{int} = 0.0519, R_{sigma} = 0.0329]
Data / restraints / parameters	8226 / 9 / 561
Goodness-of-fit on F^2	1.031
Final R indexes [$I >= 2\sigma(I)$]	R_1 = 0.0501, $_wR_2$ = 0.1377
Final R indexes [all data]	R_1 = 0.0509, $_wR_2$ = 0.1384
Largest diff. peak / hole / e Å^{-3}	1.64 / -1.03

$R_1 = \sum||F_o|-|F_c||/\sum|F_o|$. $wR_2 = [\sum w(F_o^2 - F_c^2)^2/\sum w(F_o^2)^2]^{1/2}$

Table S5 Selected Bond Distances for **2**

Bond	Length/Å	Bond	Length/Å
Cd1-O1	2.183(2)	Cd1-O5[1]	2.326(3)
Cd1-O6[1]	2.534(3)	Cd1-O7	2.371(3)
Cd1-O8	2.365(3)	Cd1-O9	2.517(2)
Cd1-O10	2.326(2)		

Table S6 Selected Bond Angles for **2**

Bonds	Angle /°	Bonds	Angle /°
O1-Cd1-O5[1]	99.02(12)	O1-Cd1-O6[1]	87.87(11)
O1-Cd1-O7	104.29(11)	O1-Cd1-O8	158.92(12)
O1-Cd1-O9	88.87(10)	O1-Cd1-O10	89.84(10)
O5[1]-Cd1-O6[1]	53.26(11)	O5[1]-Cd1-O7	85.16(11)
O5[1]-Cd1-O8	86.97(12)	O5[1]-Cd1-O9	166.64(11)
O7-Cd1-O6[1]	138.24(10)	O7-Cd1-O9	82.44(10)
O8-Cd1-O6[1]	111.52(12)	O8-Cd-O7	55.82(1`)
O8-Cd-O9	81.97(11)	O9-Cd-O6[1]	138.44(9)
O10-Cd-O5[1]	136.36(11)	O10-Cd-O6[1]	84.81(9)
O10-Cd-O7	133.92(10)	O10-Cd-O8	99.76(11)
O10-Cd-O9	53.75(8)		

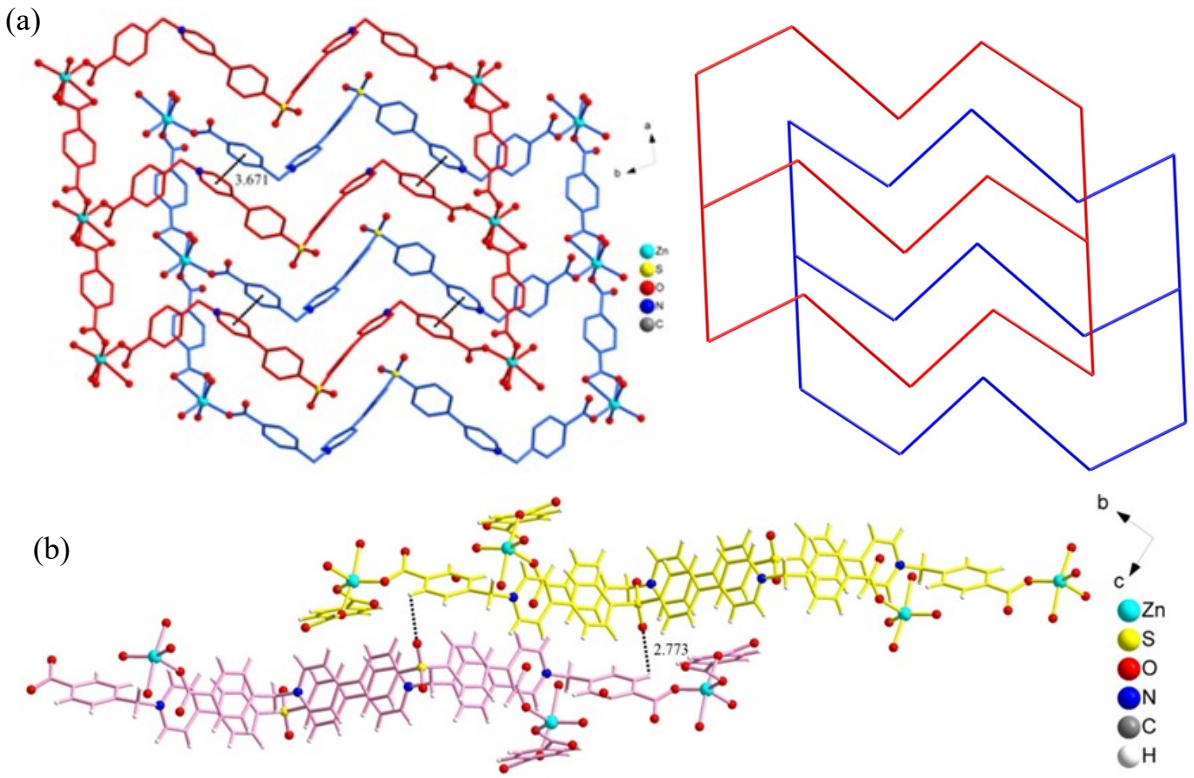

Figure S1 (a) AB stacking mode of compound **1** through π···π interactions; (b) ABAB stacking mode through (Ar)C-H···O hydrogen bonds. For clarity, parts of hydrogen atoms are omitted.

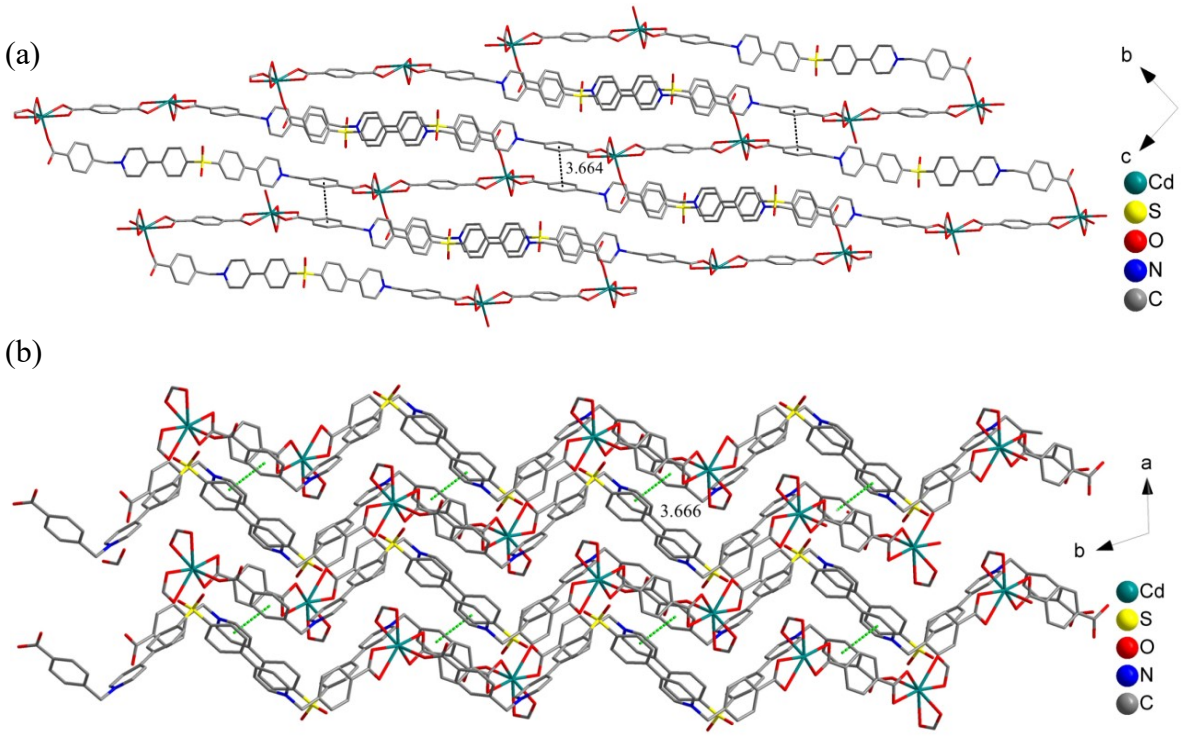

Figure S2 (a) π···π interactions of compound **2**; (b) 3D Packing pattern. For clarity, all hydrogen atoms are omitted.

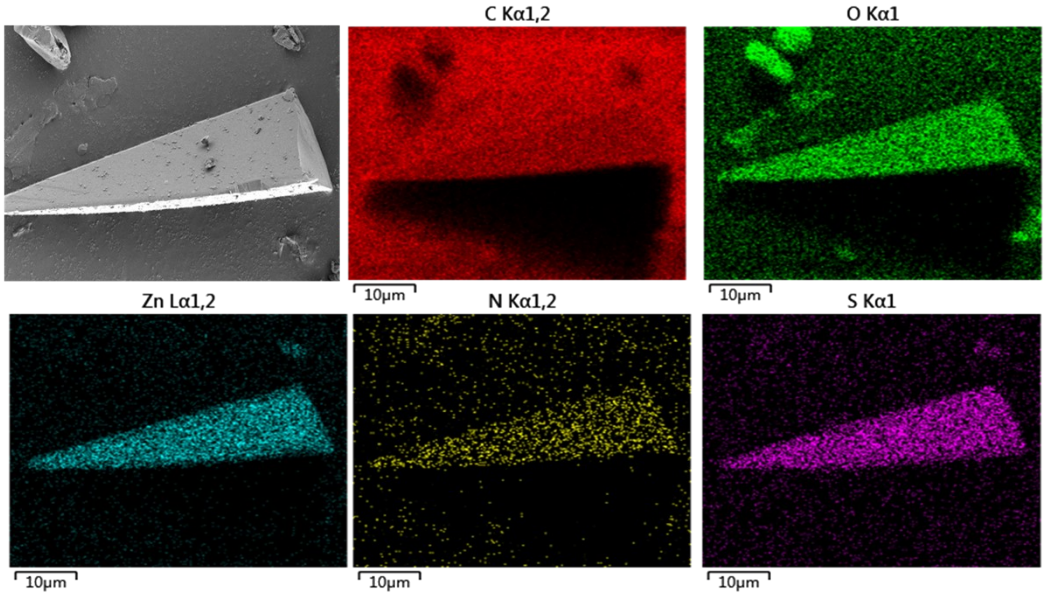

Figure S3 SEM image and mapping of **1**.

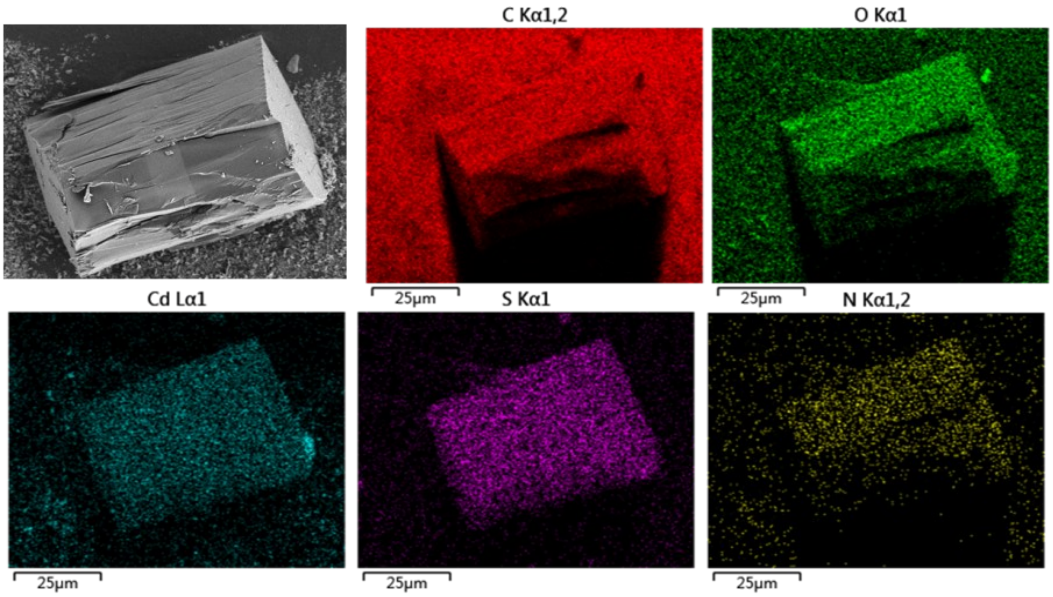

Figure S4 SEM image and mapping of **2**.

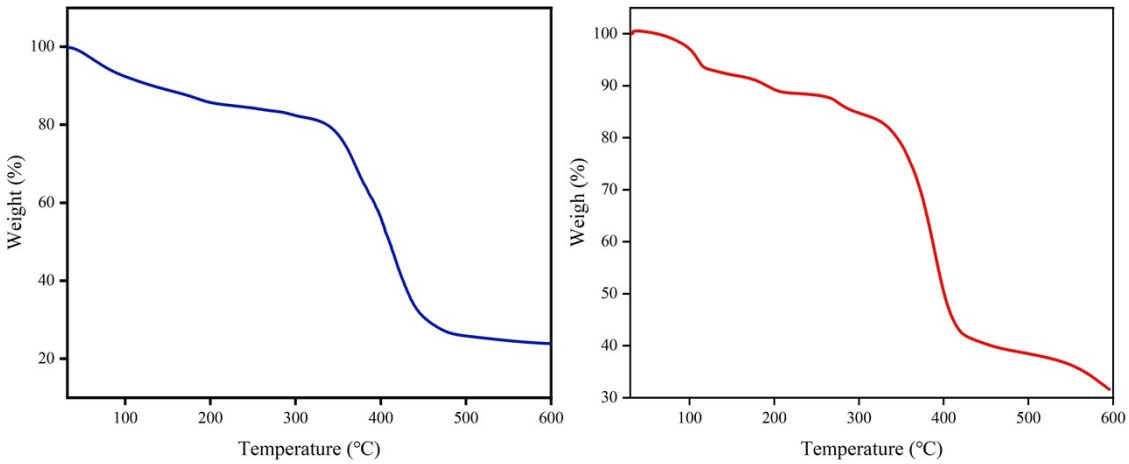

Figure S5 Thermogravimetric curves of **1** (left) and **2** (right).

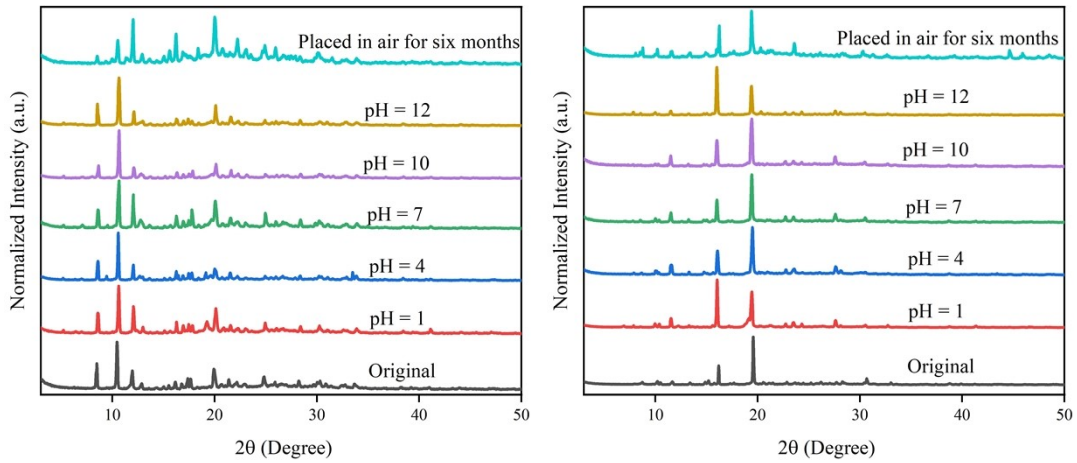

Figure S6 PXRD patterns of compounds **1** (left) and **2** (right) after treatments at different pH values and after long-term placed in air.

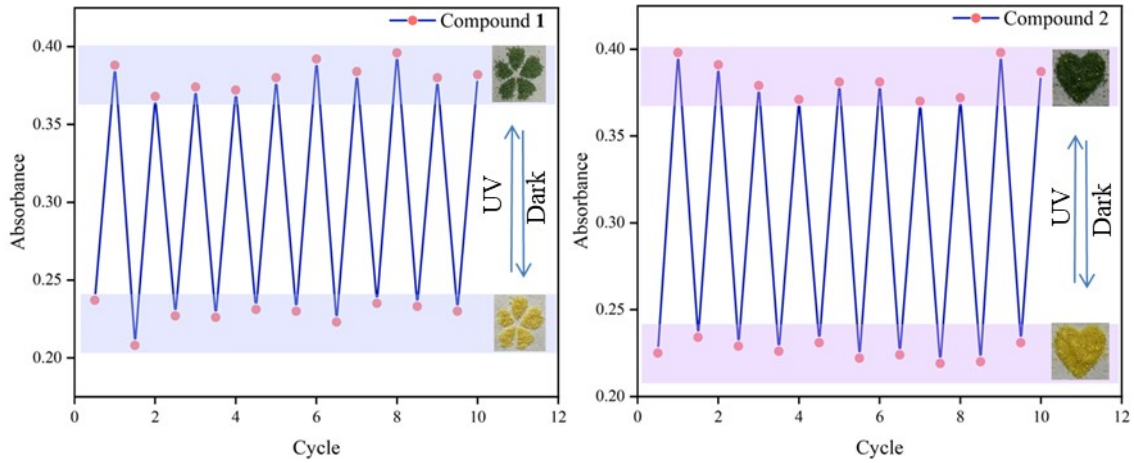

Figure S7 Stability of compounds **1** (left) and **2** (right) over 10 consecutive coloration-decoloration cycles.

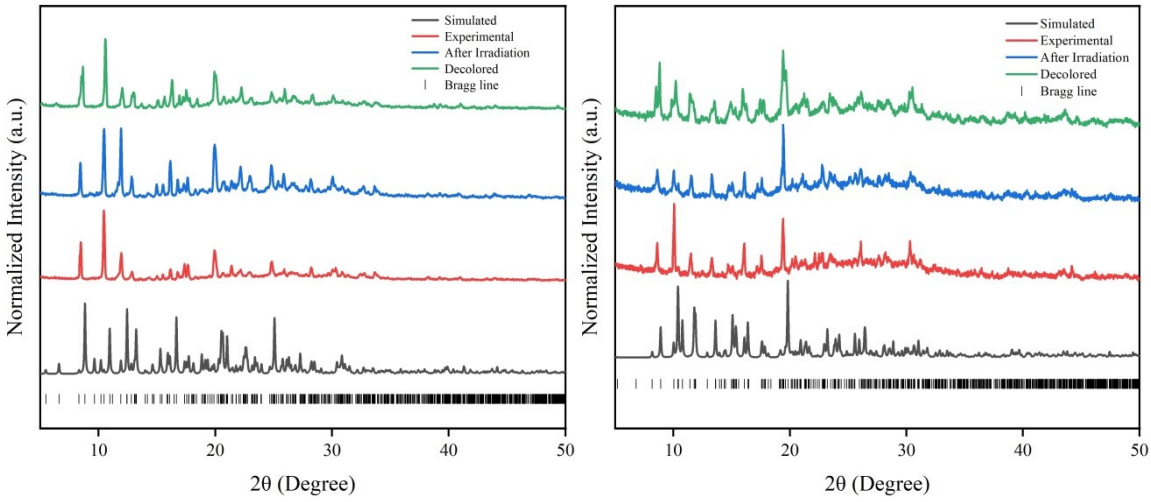

Figure S8 PXRD patterns of **1** (left) and **2** (right).

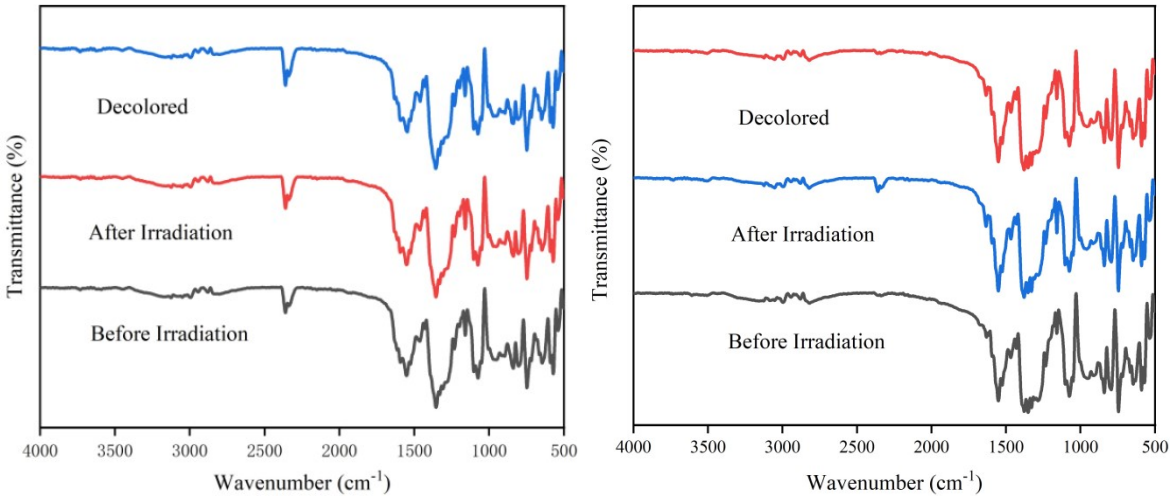

Figure S9 IR spectra of **1** (left) and **2** (right) before/after irradiation and decolored.

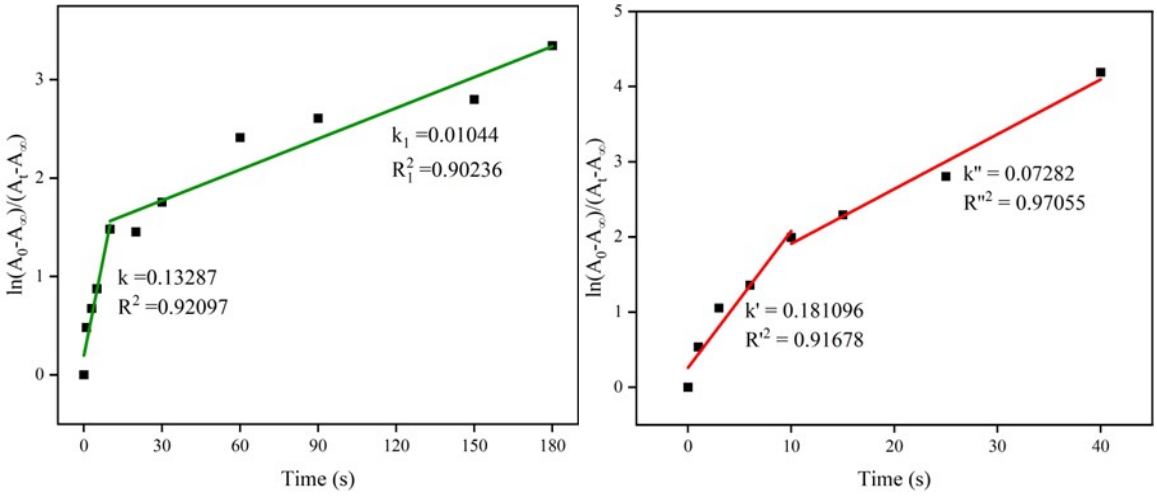

Figure S10 Photo-response kinetics on absorption at 620 nm of **1** (left) and **2** (right).

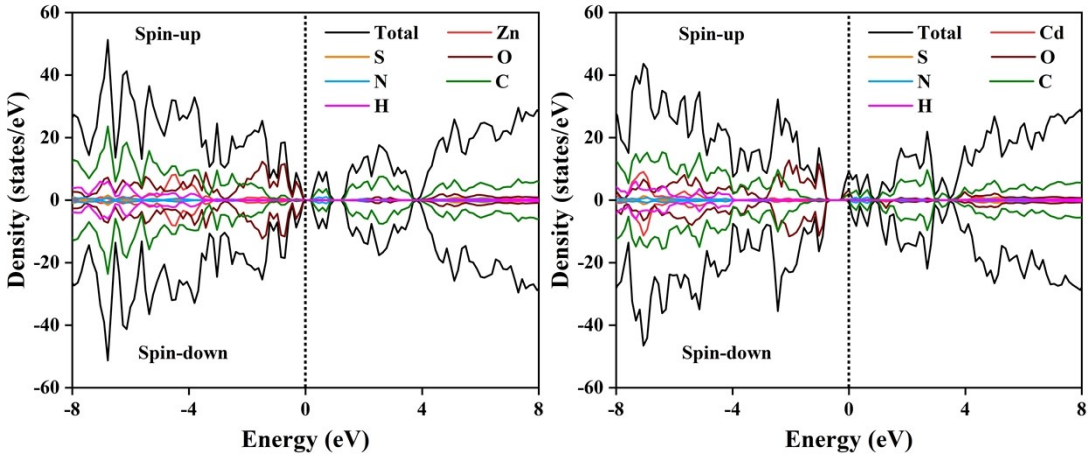

Figure S11 Total and partial density of states (DOS) of **1** (left) and **2** (right). The dashed lines represent the Fermi level.

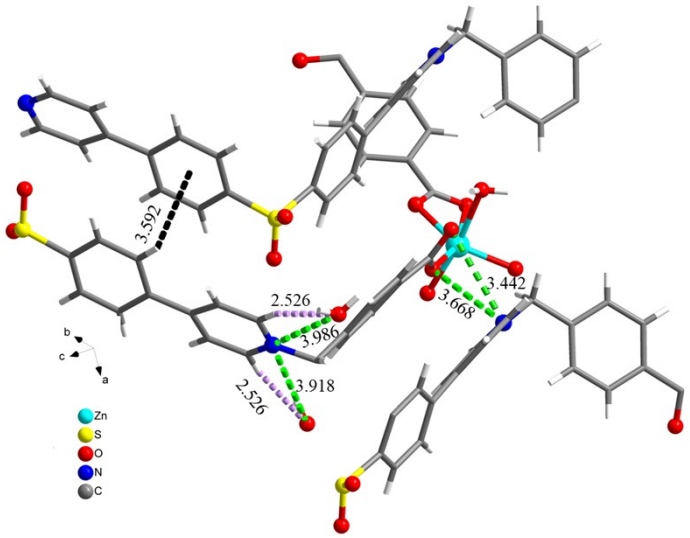

Figure S12 Potential electron transfer pathways in compound **1**. (Black: C-H···π; Green: N···O; Purple: Hydrogen bond.)

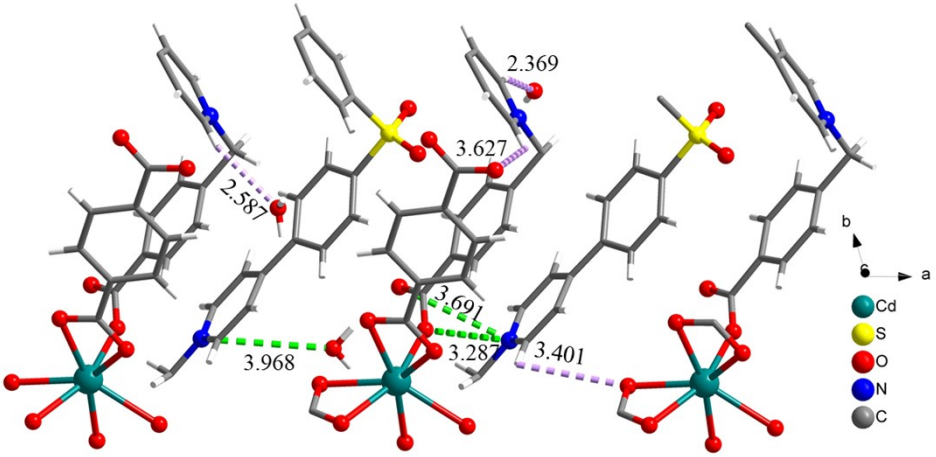

Figure S13 Potential electron transfer pathways in compound **2**. (Black: C-H···π; Green: N···O; Purple: Hydrogen bond.)

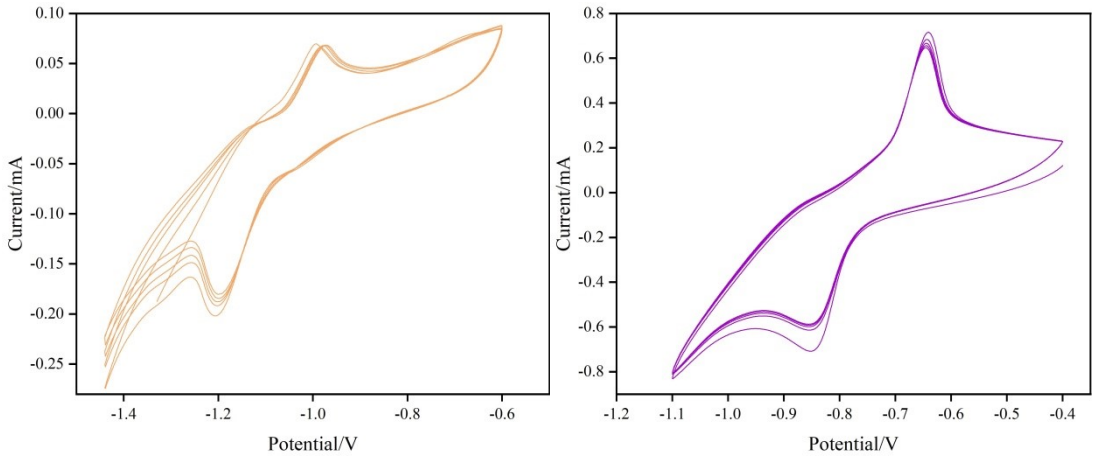

Figure S14 Cyclic voltammograms of compounds **1** (left) and **2** (right) recorded for five consecutive cycles

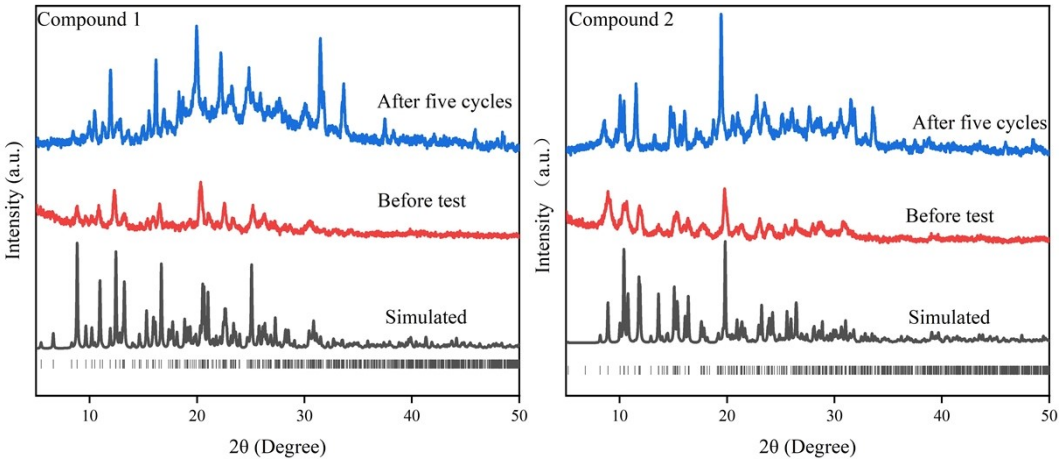

Figure S15 PXRD patterns of **1** (left) and **2** (right) before and after electrochromic switching.

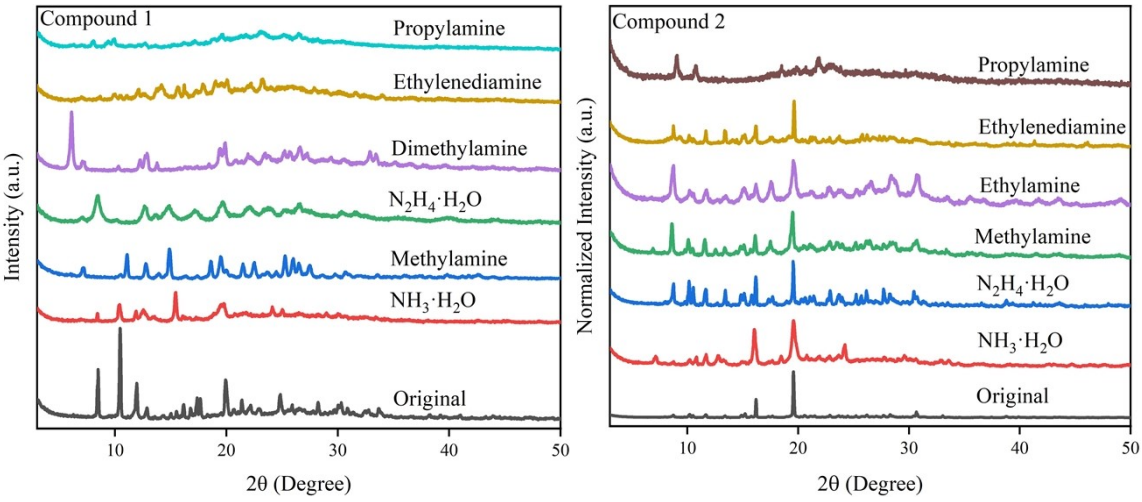

Figure S16 PXRD patterns of **1** (left) and **2** (right) in different amine vapors.

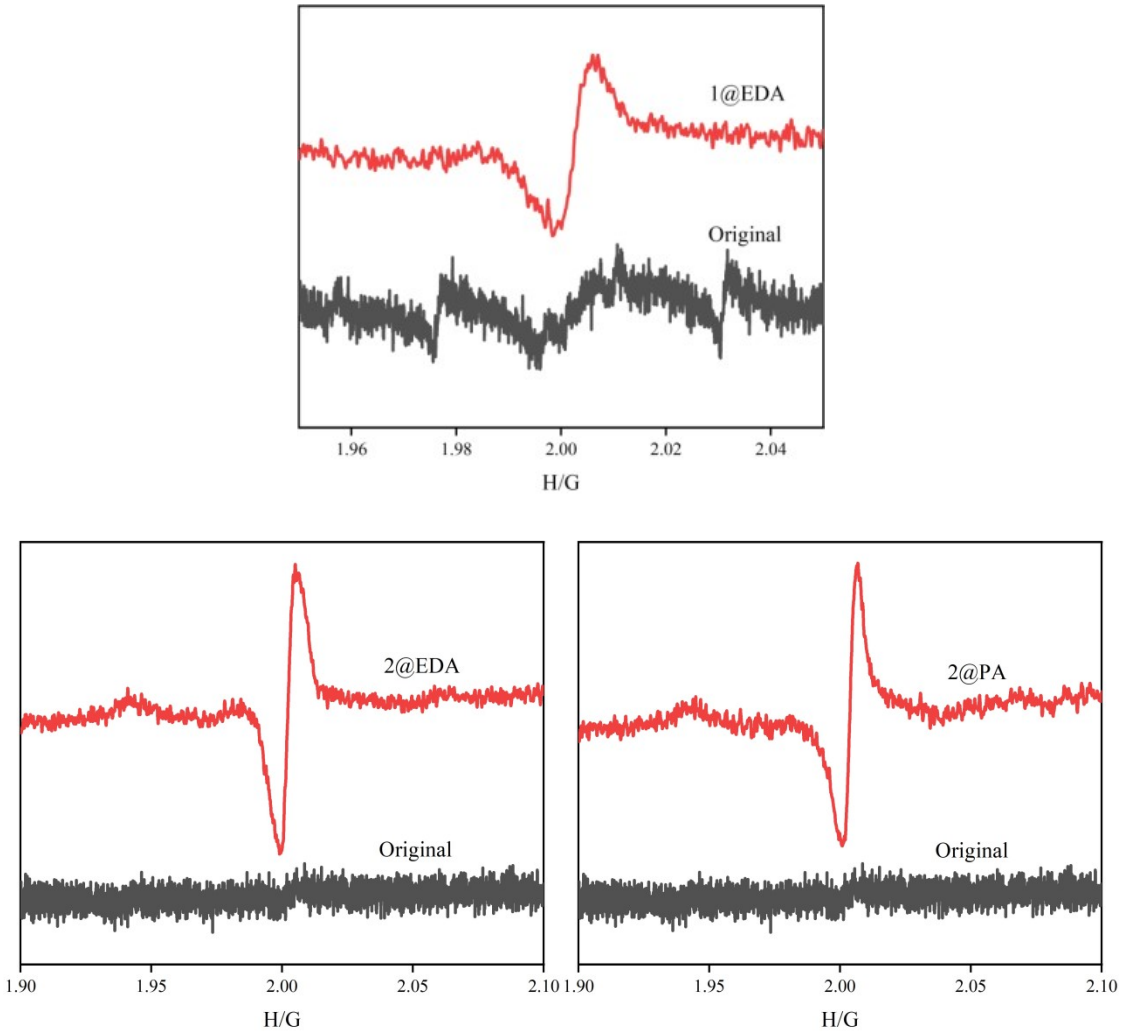

Figure S17 EPR spectra of **1** and **2** in EDA and PA vapors, respectively.

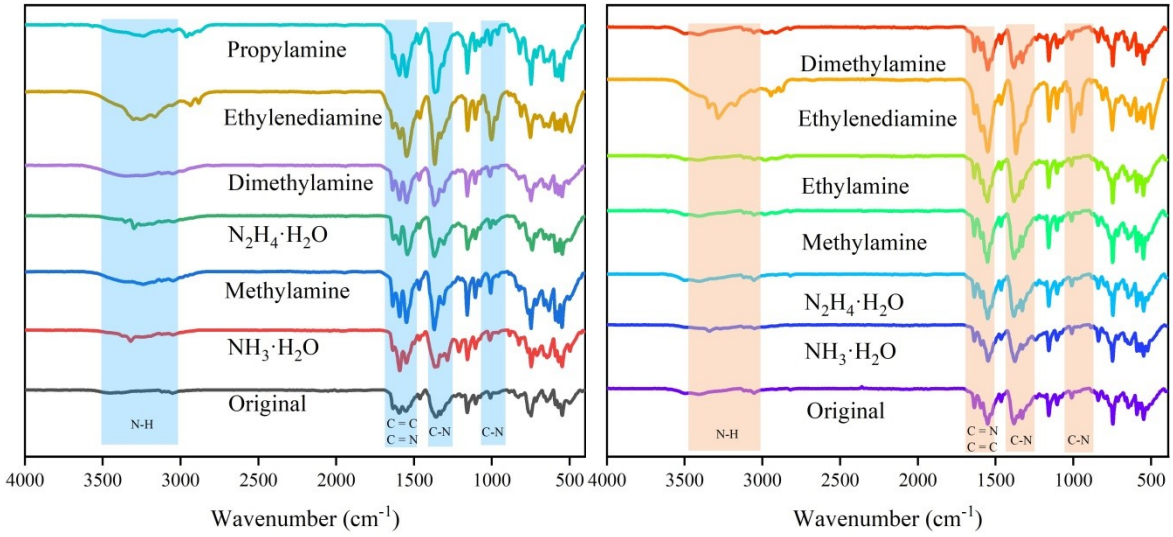

Figure S18 IR spectra of **1** (left) and **2** (right) in different amine vapors.

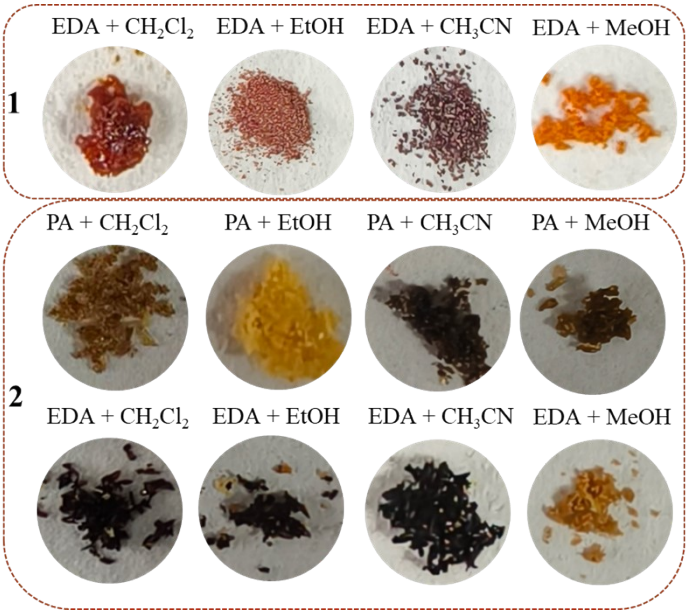

Figure S19 Photographs of compounds **1** and **2** upon exposure to EDA or PA vapors under different solvent interference conditions.

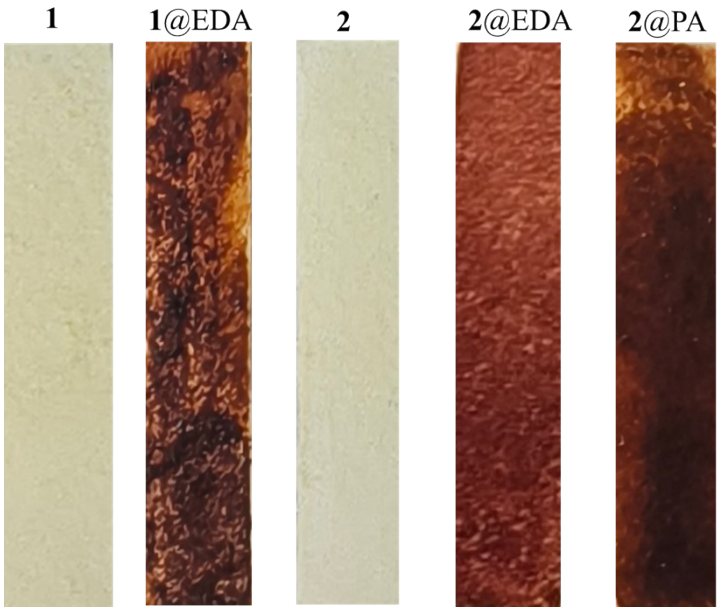

Figure S20 Photographs of test paper after fuming with EDA or PA vapors.

Supplementary References

(S1) Sheldrick, G. M. Acta Crystallogr., Sect. A: Fundam. Crystallogr., **1990**, 46, 457; Sheldrick, G. M. SHELXS-97, Program for solution of crystal structures, University of Göttingen, Germany, **1997**.

(S2) Sheldrick, G. M. SHELXL-97, Program for refinement of crystal structures, University of Göttingen, Germany, **1997**.

(S3) van der Sluis, P.; Spek, A. L. BYPASS: an effective method for the refinement of crystal structures containing disordered solvent regions. Acta Crystallographica Section A 1990, 46 (3), 194-201.

(S4) Perdew, J. P.; Burke, K.; Ernzerhof M. Generalized Gradient Approximation Made Simple. Phys. Rev. Lett. 1996, 77, 3865-3868.

(S5) Kresse, G.; Furthmüller, J. Efficiency of Ab-initio Total Energy Calculations for Metals and Semiconductors Using a Plane-Wave Basis Set. Comp. Mater. Sci. 1996, 6, 15-50.

(S6) Kresse, G.; Hafner, J. Ab initio Molecular Dynamics for Liquid Metals. Phys. Rev. B 1993, 47, 558-561.

(S7) Kresse, G.; Hafner, J. Ab initio Molecular-Dynamics Simulation of the Liquid-Metal–Amorphous-Semiconductor Transition in Germanium. Phys. Rev. B 1994, 49, 14251-14269.

(S8) Kresse, G.; Furthmüller, J. Efficient Iterative Schemes for Ab Initio Total-Energy

Calculations Using a Plane-Wave Basis Set. Phys. Rev. B 1996, 54, 11169-11186.

(S9) Monkhorst, H. J.; Pack, J. D. Special Points for Brillouin-Zone Integrations. Phys. Rev. B 1976, 13, 5188-5192.

(S10) Grimme, S. Semiempirical GGA-type Density Functional Constructed with A Long-Range Dispersion Correction. J. Comput. Chem. 2006, 27, 1787–99.

(S11) Grimme, S.; Antony J.; Ehrlich S.; Krief H. A Consistent and Accurate Ab Initio Parametrization of Density Functional Dispersion Correction (DFT-D) for the 94 elements H–Pu. J. Chem. Phys. 2010, 132,154104.